J Mater Sci (2010) 45:1350–1353
DOI 10.1007/s10853-009-4090-7

Microstructures formed during devitrification of $Na_2O{\cdot}Al_2O_3{\cdot}B_2O_3{\cdot}SiO_2{\cdot}Fe_2O_3$ glasses

Ruzha Harizanova · Günter Völksch · Christian Rüssel

Received: 24 July 2009 / Accepted: 25 November 2009 / Published online: 9 December 2009

Abstract Soda alumina borosilicate glasses of composition $(24\text{-}y)Na_2O{\cdot}yAl_2O_3{\cdot}14B_2O_3{\cdot}37SiO_2{\cdot}25Fe_2O_3$, $y = 8$, 12, 14, 16 mol%, were melted using Fe_2O_3 as raw material. Besides, samples with $y = 12$ and Fe_2O_3 concentrations of 14.32, 17.8, and 25.0 mol% were prepared from $FeC_2O_4{\cdot}2H_2O$ as raw material. The X-ray diffraction analyses showed the presence of magnetite for the samples from all the investigated compositions. Transmission electron microscopy (TEM) evidenced that all the samples are phase separated and droplets in the diameter range 100–1000 nm, enriched in iron, are formed. Inside these droplets, numerous small magnetite particles, with size in the 25–40 nm interval, are crystallized.

Abbreviations

XRD	X-ray diffraction
SEM	Scanning electron microscopy
TEM	Transmission electron microscopy
EDX analysis	Energy dispersive micro X-ray analysis
JCPDS	Joint Committee on Powder Diffraction Standards

R. Harizanova (✉)
Physics Department, University of Chemical Technology and Metallurgy, Kl. Ohridski Blvd. 8, 1756 Sofia, Bulgaria
e-mail: ruza_harizanova@yahoo.com

R. Harizanova · G. Völksch · C. Rüssel
Otto-Schott-Institut, Universität Jena, Fraunhoferstr. 6, 07743 Jena, Germany

Introduction

In the past decade, numerous reports on phase separation and crystallization phenomena in iron-rich silicate systems have been published [1]. Phase separation in the ternary system $Na_2O{\cdot}SiO_2{\cdot}B_2O_3$ is well known [2–7] and has found practical applications due to the high thermal and chemical resistance of the obtained materials [2, 4, 8]. An interpenetrating microstructure, composed of a SiO_2- and a Na_2O/B_2O_3-rich glassy phase, is usually obtained. After appropriate chemical treatment, the latter is dissolved and a porous, SiO_2-rich (95–98 wt%) material is obtained, which can be used as filters, catalyst carriers, or after sintering, as substitute of SiO_2 glass. In wide concentration range, it has been reported that the addition of Fe_2O_3 to the ternary sodium borosilicate system results in phase separation and subsequent crystallization of different iron-bearing phases, including magnetite [2].

The addition of alkaline earths or Al_2O_3, as intermediate oxides in the glass network [3–7], to the ternary sodium borosilicate system, changes the structure and the properties of glasses. It is established that in alkali-alumosilicate ternary systems, alumina, depending on its concentration, may increase the viscosity of the melt, and after some threshold concentration is reached, the viscosity decreases [8–10].

The structure and the resulting physical properties of glasses from quaternary systems containing Al_2O_3, Na_2O, B_2O_3, and SiO_2, are also well known [5–7]. In the per-alkali range ($[Na_2O] > [Al_2O_3]$) of the system $Na_2O{\cdot}Al_2O_3{\cdot}B_2O_3{\cdot}SiO_2$, the melt viscosity increases and the crystallization tendency decreases with increasing the alumina concentration [5, 7]. For equal concentration of sodium and aluminum oxide, i.e., $[Na_2O]/[Al_2O_3] = 1$, the highest viscosity is reported [7]. However, a further increase of

[Al_2O_3] results again in a decrease of the melt viscosity and in an increase of the crystallization tendency [7].

The addition of large amounts of Fe_2O_3 to the quaternary system $Na_2O{\cdot}Al_2O_3{\cdot}B_2O_3{\cdot}SiO_2$ is interesting in the light of the numerous investigations from the past two decades, especially with respect to the utilization of natural minerals or wastes for the production of glassy or glass–ceramic materials that find application as building materials, refractories, and for the preparation of pigments [1, 11]. The effect of iron oxides on the microstructure in the reported systems has been also studied [11–13]. In silicate glasses, iron oxides, mainly magnetite, usually crystallize as large dendrites. In contrast, in some rapidly quenched $Na_2O{\cdot}Fe_2O_3{\cdot}CaO{\cdot}B_2O_3$ glasses, nanocrystalline magnetite was crystallized in a subsequent annealing step [12, 13]. After dissolution of the borate glass matrix, superparamagnetic particles are observed, which might be utilized, e.g., for the preparation of ferrofluids [14, 15].

This article provides a study on the phase separation and crystallization, as well as the resulting phase formation and microstructure of glasses in the $Na_2O{\cdot}Al_2O_3{\cdot}B_2O_3{\cdot}SiO_2{\cdot}Fe_2O_3$ system.

Experimental

Glasses of composition $(24\text{-}y)Na_2O{\cdot}yAl_2O_3{\cdot}14B_2O_3{\cdot}37SiO_2{\cdot}25Fe_2O_3$, $y = 8$, 12, 14, 16 mol%, were melted under oxidizing conditions using Fe_2O_3 as raw material. In addition, samples with $y = 12$ and Fe_2O_3 concentrations of 14.32, 17.8, and 25.0 mol% were prepared from $FeC_2O_4.2H_2O$ as raw material. The latter samples are further denoted as "reduced." Raw materials used in the present investigation were: Na_2CO_3, $Al(OH)_3$, $B(OH)_3$, SiO_2, Fe_2O_3, and $FeC_2O_4{\cdot}2H_2O$. Glasses prepared from Fe_2O_3 were melted in 150 g batches at 1400 °C for 1.5 h in air, using an inductive furnace and Pt-crucibles. The melts were subsequently quenched between Cu-blocks. The reduced compositions were prepared in batches of 75 g and melted in silica crucibles for 0.5–2.5 h at 1400 °C in a $MoSi_2$ furnace in air. For faster cooling, the reduced melts were drawn to fibers. This was not possible for the oxidized melts due to their lower viscosity.

X-ray diffraction analysis (XRD) of powdered samples was used to obtain information on the phase composition of the synthesized samples. X-ray diffraction patterns (XRD-patterns) were recorded in the 10–90° interval, using an X-ray diffractometer HZG4 + ID3000 (Seifert&Co.) and FeK_α-radiation. The microstructure was investigated by means of electron microscopy (scanning electron microscope (SEM): Zeiss DSM 940A and transmission electron microscope (TEM): Hitachi H-8100). The samples were polished and coated with gold or carbon for imaging and energy-dispersive X-ray (EDX) analysis in the SEM. Replica or powdered samples were prepared for TEM.

Results

The melted glasses had black coloration and were partially crystalline. The XRD-patterns, attributed to samples with different [Na_2O]/[Al_2O_3] ratios, are shown in Fig. 1. The crystalline phase formed for all studied [Na_2O]/[Al_2O_3] ratios is magnetite (JCPDS-Nr. 86-1352). In Fig. 2, the XRD-pattern of a reduced sample with 25 mol% Fe_2O_{3-x}

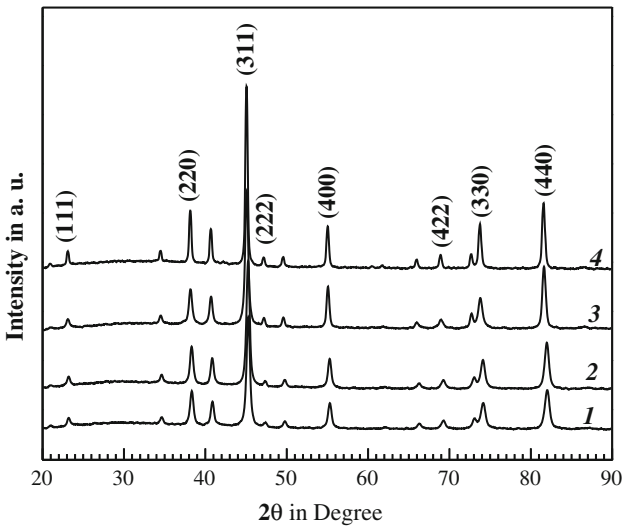

Fig. 1 XRD-patterns of samples with the compositions $(24\text{-}y)Na_2O{\cdot}yAl_2O_3{\cdot}14B_2O_3{\cdot}37SiO_2{\cdot}25Fe_2O_3$, where 1: $y = 8$; 2: $y = 12$; 3: $y = 14$; 4: $y = 16$ mol%

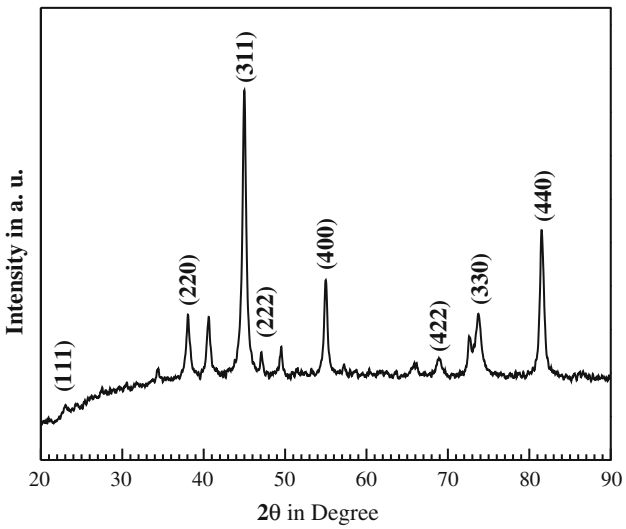

Fig. 2 XRD-pattern of a reduced sample with composition $12Na_2O{\cdot}12Al_2O_3{\cdot}14B_2O_3{\cdot}37SiO_2{\cdot}25Fe_2O_{3-x}$

is shown. In analogy to the oxidized samples, magnetite is again the only detected crystalline phase. Besides, the glass halo can be seen in the 2θ-range from 20 to 40°. Small peaks at 34° and 66° were found in all the XRD-patterns, which could not be attributed to any identifiable crystalline phase. The peaks at 40.5° and 72.5° could not be identified as magnetite, according to JCPDS-Nr. 86-1352, but may be attributed to other modifications of the same phase (JCPDS-Nr. 89-951 and 3-863). The peak at 49° could be assigned to maghemite (JCPDS-Nr. 89-5892), which, however, is not very reliable since the relative intensities of the peaks at 33° and 49° do not correspond to those given in the JCPDS database.

The microstructure of all obtained samples, as studied using SEM and TEM, shows the existence of phase separation (see Fig. 3). The phase-separated and subsequently crystallized regions are droplet-like with sizes varying from 100 to 1000 nm. In Figs. 4 and 5, TEM micrographs are shown, which were obtained from fine powdered drawn to fibers samples. Similarly to Fig. 3, spherical inclusions are observed. The same droplet-like structures are also observed for all the other reduced and nonreduced samples. Each droplet contains cubic crystals which, according to the XRD-patterns, consist of magnetite. The sizes of the cubic magnetite crystals are in the range from 25 to 40 nm, which is in rough agreement with crystallite sizes calculated from Scherrer Equation (25 nm). The crystal volume fraction for the sample from Fig. 3, as determined from the SEM micrograph, was (49 ± 3)%. It may be stated from

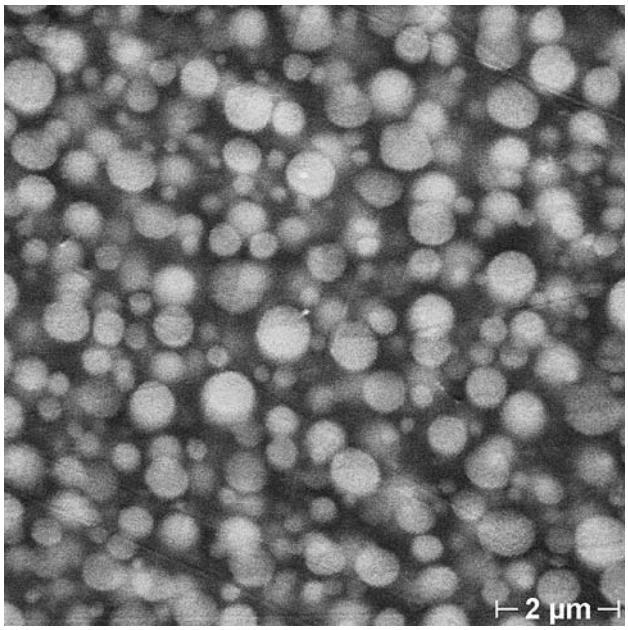

Fig. 3 SEM-micrograph of a sample with composition $8Na_2O{\cdot}16Al_2O_3{\cdot}14B_2O_3{\cdot}37SiO_2{\cdot}25Fe_2O_3$

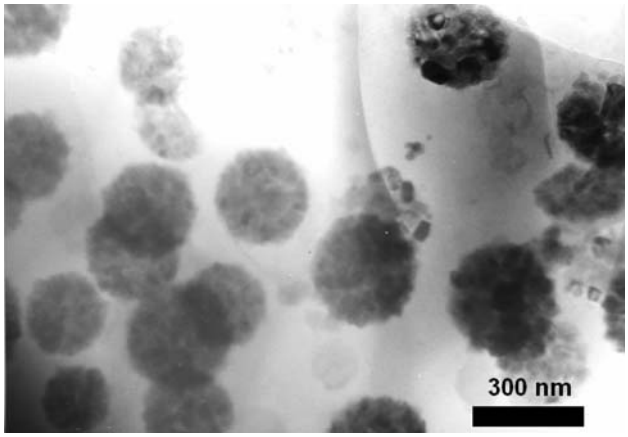

Fig. 4 TEM-micrograph of a powdered fiber with the reduced composition $13.75Na_2O{\cdot}13.75Al_2O_3{\cdot}15.96B_2O_3{\cdot}42.22SiO_2{\cdot}14.32Fe_2O_{3-x}$

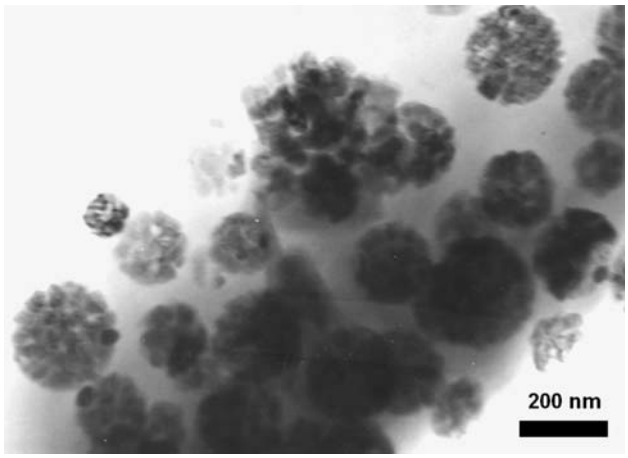

Fig. 5 TEM-micrograph of a powdered fiber with the reduced composition $12Na_2O{\cdot}12Al_2O_3{\cdot}14B_2O_3{\cdot}37SiO_2{\cdot}25Fe_2O_{3-x}$

Figs. 4 and 5 that the average size of the droplets in the reduced samples with 14.3 and 25.0 mol% Fe_2O_{3-x} does not significantly differ. However, the number of the droplets seems to be larger for the sample with 25 mol% Fe_2O_{3-x} in comparison to that with 14.32 mol%.

Discussion

All the samples studied were partially crystallized and showed magnetite as the only crystalline phase attributable to the XRD-patterns. Besides, considerable quantities of residual glassy phase are present as is seen in the XRD-patterns (glass halo) and in the micrographs. The intensities of the respective peaks in the XRD-pattern are slightly different, which could be an effect of the different sample preparation procedures, resulting in possible different crystallographic orientation and/or nonstoichiometry.

Despite the variation of the $[Na_2O]/[Al_2O_3]$ ratio, phase separation and crystallization of magnetite was observed for all the investigated compositions. Substituting the raw material Fe_2O_3 against FeC_2O_4 leads to an increasing $[Fe^{2+}]/[Fe^{3+}]$ ratio and to an additional increase in the melt viscosity. Thus, the use of FeC_2O_4 instead of Fe_2O_3 as raw material in this study enabled fiber drawing and hence much larger cooling rates. This resulted in smaller sizes of the formed droplet-like structures. The increased viscosity of the melt and the decrease of the droplets sizes are beneficial since the smaller the formed structures, the easier the further processing of the resulting specimens.

The droplets have sizes from 100 to 1000 nm and volume fraction of about 50% (see "Results" section). It should be assumed that liquid/liquid phase separation occurs first in the melt, as already observed for similar iron-containing systems [1] and droplets, whose dark appearance is due to their enrichment in iron, are formed. Subsequently, inside the droplets, complex structures containing cubic crystalline magnetite are formed. The formation of magnetite crystals was also observed by other authors, [11–13]. However, in the present case, spinodal decomposition and dendritic crystal growth were not observed, in contrast to the results reported in [11]. This should allow an easier separation of the formed magnetite crystals from the glass matrix and possibly their utilization for the production of magnetic ferrofluids or inks [14, 15]. It should be noted (as reported in [12, 13]) that roller quenching of borate glasses with high iron concentrations and subsequent annealing, leads to magnetite nanocrystals with sizes from 15 to 25 nm. However, those crystals are uniformly distributed in the glass matrix and are superparamagnetic [12]. During the course of phase separation, the concentration of iron in the matrix phase decreases. This should lead to a decrease in the viscosity, as reported for borate glasses containing high iron concentrations [13]. This decrease in the viscosity should decelerate the crystallization of the glassy matrix phase, while the crystallization of the droplet phase should be enhanced by the high iron concentrations. The same behavior is observed in our investigations of glasses in the system $Na_2O{\cdot}Al_2O_3{\cdot}B_2O_3{\cdot}SiO_2{\cdot}Fe_2O_3$.

The crystallization of other iron containing phases, such as hematite (Fe_2O_3), was never observed, even in the oxidized samples, i.e., in those prepared from Fe_2O_3 as raw material.

Conclusions

In the studied glass system, phase separation occurs. Droplets with sizes in the 100–1000 nm range enriched in iron and containing crystalline magnetite with crystallite sizes in the 25–40 nm range are formed in an amorphous matrix. The different $[Na_2O]/[Al_2O_3]$ ratios did not change the phase composition and the microstructure of the synthesized samples, although they affected the viscosity of the melt and the volume fraction of the formed magnetite crystals. The variation of the iron oxide concentration results in a slight change of the droplet sizes, but it does not lead to changes in the type of the crystallizing phase.

References

1. Karamanov A, Pelino M (2001) J Non-Cryst Solids 281:139
2. Ehrt D, Reiß H, Vogel W (1976) Silikattechnik 27:304
3. Kingery WD, Bowen HK, Uhlmann DR (1991) Introduction to ceramics. Wiley, Singapore
4. Kunath-Fandrei G, Ehrt D, Jäger C (1995) Z Naturforsch 50a:413
5. El-Egili K (2003) Phys B 325:340
6. Hornschuh S, Messerschmidt B, Possner T, Possner U, Rüssel C (2004) J Non-Cryst Solids 347:121
7. Hong L, Hrma P, Vienna JD, Qian M, Su Y, Smith DE (2003) J Non-Cryst Solids 331:202
8. Benne D, Rüssel C, Menzel M, Becker K (2004) J Non-Cryst Solids 337:232
9. Schirmer H, Keding R, Rüssel C (2004) J Non-Cryst Solids 336:37
10. Benne D, Rüssel C, Niemer D, Menzel M, Becker KD (2004) J Non-Cryst Solids 345–346:203
11. Romero M, Rincon JM (1999) J Am Ceram Soc 82:1313
12. Woltz S, Hiergeist R, Görnert P, Rüssel C (2006) J Magn Magn Mater 298:7
13. Woltz S, Rüssel C (2004) J Non-Cryst Solids 337:226
14. Odenbach S (2004) J Phys Condens Matter 16:1135
15. Zhou GY et al (2004) Smart Mater Struct 13:309